Title

Evidence for the organization of chromatin in megabase pair-sized loops arranged along a random walk path in the human G0/G1 interphase nucleus.

Journal

Journal of Cell Biology, 130(6)

ISSN

0021-9525

Authors

Yokota, H
van den Engh, G
Hearst, JE
et al.

Publication Date

1995-09-15

DOI

10.1083/jcb.130.6.1239

Peer reviewed

Evidence for the Organization of Chromatin in Megabase Pair–sized Loops Arranged along a Random Walk Path in the Human G0/G1 Interphase Nucleus

Hiroki Yokota,* Ger van den Engh,* John E. Hearst,‡ Rainer K. Sachs,§ and Barbara J. Trask*

*Department of Molecular Biotechnology, University of Washington, Seattle, Washington 98195; and Departments of ‡Chemistry and §Mathematics, University of California, Berkeley, California 94720

Abstract. We determined the folding of chromosomes in interphase nuclei by measuring the distance between points on the same chromosome. Over 25,000 measurements were made in G0/G1 nuclei between DNA sequences separated by 0.15–190 megabase pairs (Mbp) on three human chromosomes. The DNA sequences were specifically labeled by fluorescence in situ hybridization. The relationship between mean-square interphase distance and genomic separation has two linear phases, with a transition at ~2 Mbp. This biphasic relationship indicates the existence of two organizational levels at scales >100 kbp. On one level, chromatin appears to be arranged in large loops several Mbp in size. Within each loop, chromatin is randomly folded. On the second level, specific loop-attachment sites are arranged to form a supple, backbonelike structure, which also shows characteristic random walk behavior. This random walk/giant loop model is the simplest model that fully describes the observed large-scale spatial relationships. Additional evidence for large loops comes from measurements among probes in Xq28, where interphase distance increases and then locally decreases with increasing genomic separation.

SHORTLY after cell division, the mitotic chromosomes decondense and diffuse into the interphase nucleus. While individual chromosomes cannot be discerned, important processes related to chromosome function take place. Regulatory factors interact with chromatin, DNA is made accessible for transcription, RNA is produced and processed, DNA is replicated, and repairs are made of DNA strand breaks. When the chromosomes reappear for the next mitosis, they have been duplicated and prepared for rapid partitioning over the daughter cells. The complexity of these processes raises many questions about the large-scale organization of chromosomes and how this organization relates to cell function (e.g., Blobel, 1985; Manuelidis and Chen, 1990; Cook, 1991; Lawrence and Singer, 1991; De Boni, 1994).

Diverse models, ranging from highly random to highly organized, have been proposed for the higher-order organization of interphase chromatin. These models variously involve irregularly folded fibers (DuPraw, 1965), radial loop structures (Manuelidis and Chen, 1990), giant loops (Ostashevsky and Lange, 1994), semirigid orientation ("Rabl" configuration) (Rabl, 1885; Comings, 1968), or random polymers confined by tethering or external forces (Hahnfeldt et al., 1993). Some models assign to chromosomal organization a dominant role in cell function. Cremer et al. (1993) suggested that gene-rich and early-replicating chromatin is systematically organized so that it is readily accessible to the transcription and replication machinery. Using elegant optical techniques, Sedat and coworkers demonstrated a systematic arrangement of *Drosophila* prometaphasic chromosomes, with telomeres and centromeres located at opposite nuclear poles (Hiraoka et al., 1990*a*). It is not clear, however, whether these observations apply to mammalian cells.

While much has been learned about chromatin structure at small scales (<100 kbp) (for reviews see van Holde, 1989; Lewin, 1994), there have been few quantitative studies on the large-scale geometry of mammalian interphase chromosomes (van den Engh et al., 1992). Consequently, it has not been possible to discriminate among the various proposals for nuclear structure.

Fluorescence in situ hybridization (FISH)[1] offers new possibilities for bringing out structural features of chromosomes within interphase nuclei. The sites of specific DNA sequences can be fluorescently marked for direct microscopic examination. Using FISH, an important discovery about interphase chromosomes was made. Probes that stain or "paint" whole chromosomes show that individual

Address all correspondence to Barbara J. Trask, Ph.D., Department of Molecular Biotechnology, Box 357730, University of Washington, Seattle, WA 98195. Tel.: (206) 685-7347. Fax: (206) 685-7354.

1. *Abbreviations used in this paper*: DAPI, 4′6,-diamidino-2-phenylindole; FISH, fluorescence in situ hybridization; hypo-MAA, hypotonic buffer, methanol/acetic acid fixative, Mbp, megabase pair.

chromosomes occupy restricted subcompartments or domains in the mammalian interphase nucleus, rather than being dispersed throughout the nuclear volume (Lichter et al., 1988; Pinkel et al., 1988). The shape of these domains is irregular and highly variable among cells. Details about the path taken by chromatin within these domains have remained obscure. The variable character of the chromosomal domains implies that systematic patterns of chromosomal organization, if they exist, can only be derived from a statistical analysis of a large number of observations.

We have developed a statistical approach to study the large-scale geometry of individual interphase chromosomes (van den Engh et al., 1992). In this approach, the folding of chromatin is inferred from the distances measured between two probes from known genomic sites. Measurements in one cell are inconclusive, but the pattern of folding can be revealed by repeated observations of a given probe pair in many cells and by observations of many probe pairs. The relative positions of two small (~40-kbp) DNA sequences are determined in large numbers of nuclei. One probe's site is labeled by FISH with a green fluorochrome, and the second probe's site is labeled with a red fluorochrome. The separation, in basepairs, of these sequences along the DNA molecule is known. Sites separated by 50 kbp or more are resolved in interphase nuclei by using conventional fluorescence microscopy (Trask et al., 1989*a*). Thus, chromatin folding at scales >50 kbp can be analyzed with this technique.

Using this approach, we showed previously that over relatively short (0.1 to ~2 Mbp) genomic separations interphase chromatin exhibits the random walk behavior typical of linear polymers (van den Engh et al., 1992). Linear polymers can be considered as long, flexible molecular chains that fold in a random manner. The statistical properties of such chains are well studied. The overall length and shape of a folded chain are accurately described by statistical methods based on random walk models (Cantor and Schimmel, 1980; Doi and Edwards, 1988; Flory, 1988). One hallmark of random walk, polymer behavior is that the mean-square projected two-dimensional distance between points on a chain in its random conformations is linearly proportional to the separation between the points on the straightened chain, d,

$$\langle r^2 \rangle \propto d$$

where r represents distance between points on the randomly folded molecule, and <..> indicates mean. Using a set of probes spanning a genomic range of 50 kbp–4 Mbp, we found that chromatin chains show such random walk behavior (van den Engh et al., 1992). For genomic separations <2 Mbp, mean-square interphase distance ($<r^2>$) increases as a linear function of genomic separation (d). An additional similarity between polymers and chromatin in the range of 0.1 to ~2 Mbp was also noted in repetitive measurements of distances between two given probes. The statistical distribution of such distances also conforms to the pattern expected for polymers. Thus, on the scale of 0.1–2 Mbp, chromatin structure is dominated by random influences.

An abrupt change in the polymer-like behavior of interphase chromatin was observed around 2 Mbp (Trask et al., 1991, 1993*a*; van den Engh et al., 1992). Above this genomic separation, mean interphase distance appeared to plateau. This plateau indicated that additional constraints are acting to prevent the random dispersion of chromatin. The short distance measurements did not allow us to draw conclusions about the nature of these constraining structures, however.

In this paper, we extend our quantitative studies on the conformation of mammalian chromosomes in interphase. We present the first data relating interphase distance to genomic separation for separations up to the length of an entire chromosome. Using probes on three different human chromosomes, interphase distances were measured for 131 genome separations ranging from 0.15 to 190 Mbp. We find that the relationship between mean-square interphase distance and genomic distance has two linear phases. These two linear phases are clear indication of two different regimes of flexible chain, polymer-like behavior. Additional evidence for random walk behavior stems from our analyses of the statistics of the distance distributions. These two polymer-like regimes can be interpreted as a systematic organization of chromatin in giant loops returning to a flexible backbone. Observation of apparent inversion in probe order in the 2- to 4-Mbp range, with mean interphase distance locally decreasing as a function of genomic separation, is provided here as further evidence of a looped chromatin structure. On the basis of these findings, we propose a random walk/giant loop model for interphase chromosomes. The mathematical details of this model, based on the data presented below, are being presented elsewhere (Sachs et al., 1995).

Materials and Methods

For most of the experiments described, human normal male fibroblast cells were grown to and held at confluency without medium change for 2–4 d. Flow cytometric analyses show that these cultures contain >95% of cells in G0/G1. Nuclei were treated for 15 min at 37°C in 40 mM hypotonic KCl buffer, centrifuged, fixed three times in 3:1 methanol/acetic acid, and dropped on glass microscope slides. The nuclei were then denatured by dipping the slides in 70% formamide/2 × SSC at 72°C followed by dehydration in a series of cold ethanol. Nuclei were also prepared by two alternative procedures. The first was exactly as described above, except that the hypotonic step was omitted. The second procedure was developed by Popp et al. (1990) in an effort to better preserve nuclear organization on the scales we analyze here. Fibroblast cells were grown on coverslips, washed in PBS, fixed in 4% paraformaldehyde in PBS for 5 min, washed again in PBS, and incubated twice for 5 min in 0.1% Triton X-100 in PBS. The slides were then washed in 0.1 M Tris-HCl (pH 7.3) for 2 min, equilibrated in 20% glycerol in PBS for 20 min, and exposed to three freeze–thaw cycles by dipping in liquid nitrogen. The slides were stored at 4°C in PBS before use. To avoid any exposure to ethanol, the slides were placed in ice-cold 70% formamide/2 × SSC after denaturation. Slides prepared by all three procedures were hybridized to labeled DNA sequence probes in 50% formamide/10% dextran sulfate/2 × SSC at 37°C as described previously (Trask, 1991*a*; van den Engh et al., 1992). For each experiment, two cosmid probes, marking different chromosomal locations, were differentially labeled with biotin or digoxigenin by nick translation and hybridized simultaneously to nuclei. Probe sites were detected with different fluorochromes using avidin–Texas red and FITC-conjugated antibodies directed against digoxigenin. Nuclei were counterstained with 2 μM 4′,6-diamidino-2-phenylindole (DAPI) in a glycerol- and phenyldiamine-based antifade solution (Johnson and Noguera-Araujo, 1981).

The probes used in the study are illustrated in Fig. 1. 10 cosmids from within a 4-Mbp region of 4p16.3 were obtained from Marcy MacDonald (Massachusetts General Hospital, Boston, MA) and Gillian Bates (Imperial Cancer Research Foundation, London, UK). Cosmids representing locations within a region of ~3.5 Mbp of Xq28 were provided by Jane Gitschier (University of California, San Francisco), Jean-Louis Mandel (INSERM, Strasbourg, France), Anne-Marie Poustka (Deutsches Krebs-

forschungszentrum, Heidelberg, FRG), and Kay Davies (John Radcliffe Hospital, Oxford, UK). Cosmids containing sequences hybridizing to 10, 8, and 7 different points along chromosomes 4, 5, and 19 were obtained from Rick Myers (Stanford University, Stanford, CA), Greg Landes (Integrated Genetics, Framingham, MA), and Anthony Carrano (Lawrence Livermore National Laboratory, Livermore, CA), respectively.

Fibroblast nuclei are flattened ellipsoids, a feature that confines our analyses to two dimensions. Photography and distance measurements were performed in a blind fashion, without knowledge of the genomic separation of the hybridized probes. For each probe pair, photographs were taken of randomly selected nuclei (640T film; Scotch 3M, St. Paul, MN, exposure ~20s) using an Axiophot microscope (Carl Zeiss, Inc., Thornwood, NY) equipped with a ×100, 1.3 NA plan-Neofluar objective and a band pass filter (ChromaTechnology, Brattleboro, VT) selected to transmit Texas Red, FITC, and a slight amount of DAPI counterstain. Photographic images were projected at a magnification of ~10,000 onto a digitizing board (40 lines/mm; Summagraphics Corp., Seymour, CT). The coordinates of paired red and green hybridization were entered through the digitizing board into a computer (NeXT Computer, Inc., Palo Alto, CA) for further analysis (van den Engh et al., 1992). An average of 179 (range, 50–361) point-to-point distances was measured for each probe pair. Digital image collection was contemplated, but deemed too slow and costly for the large number of distance measurements (~25,000) and images (~4,000) needed for this study.

To assess overall nuclear morphology, the DAPI staining patterns of alternatively fixed nuclei, before and after denaturation and FISH, were compared with nuclei in unfixed cells (slightly permeabilized to DAPI with 0.02% Triton X-100) using conventional epifluorescence microscopy as well as a DeltaVision microscope and three-dimensional image processing system (Applied Precision Inc., Mercer Island, WA). Preparations were stained with 0.1 μM DAPI in antifade for 2 h. The DeltaVision system collects high resolution images (pixels 0.045–0.076 μm on a side) separated by 0.2 μm in the z-dimension and corrects these optical sections for out-of-focus information by using a deconvolution algorithm (Agard et al., 1989; Hiraoka et al., 1990*b*).

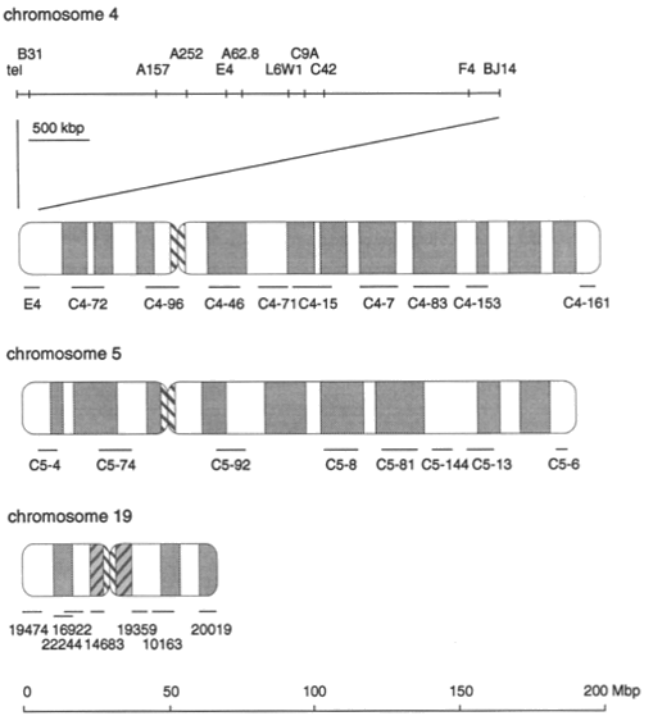

Figure 1. The locations of cosmid probes used in this study. The map of 10 probes from a 4-Mbp region at the telomere of human chromosome 4p16.3 is derived from the literature (Bates et al., 1990; Buçan et al., 1990; Lin et al., 1991; Whaley et al., 1991). Estimates of genomic separation between these probes vary by ~10%. Nine additional probes map to different sites along chromosome 4. Eight probes map to sites on human chromosome 5. The figure indicates the range of map position as determined by measuring the distance between probe hybridization site and the p terminus (chromosome 4: Myers and Goold, 1992; chromosome 5: Lu-Kuo et al., 1994) and by mapping relative to R-bands (Yokota, H., unpublished data). Seven cosmids distributed along human chromosome 19 were chosen on the basis of their map position relative to cytogenetic bands (Trask et al., 1993*b*). The DNA contents of chromosomes 4, 5, and 19 are estimated to be 200, 190, and 65 Mbp, respectively (Trask et al., 1989*b*). Conversion of differences in fractional-length measurements or band positions to Mbp are approximate with an error of ± 3–7 Mbp. Because of the uncertainty in probe location along the chromosome, a conservative estimate of the error in large genomic separation values plotted in Figs. 2–4 is ± ~10 Mbp.

Results

The Relationship of Mean-Square Interphase Distance and Genomic Separation has Two Linear Phases

Interphase distance was measured among 19 probes distributed along chromosome 4 (Fig. 1). Fig. 2 shows mean-square interphase distance, $<r^2>$, and genomic separation for 80 probe pairs representing genomic separations ranging from 0.13 to ~10 Mbp. We here plot $<r^2>$, rather than mean interphase distance $<r>$ or its square $<r>^2$, to facilitate comparison of our data to the predictions of polymer models (e.g., Cantor and Schimmel, 1980; Sachs et al., 1995).

The observed relationship for genomic separations >10 Mbp has several notable features. (*a*) $<r^2>$ increases linearly with genomic separation. (*b*) The slope of the relationship is significantly positive (0.08 μm²/Mbp). (*c*) The best-fit linear regression line intersects the *y*-axis at ~2.5 μm². (*d*) The spread of the data points around the regression line is roughly constant across the entire genomic separation range (~1.5 μm²).

The slope of data points for genomic separations <4 Mbp differs markedly from the slope observed for probes >10 Mbp apart. The short distance measurements confirm our earlier findings on different nuclear preparations (van den Engh et al., 1992) and allow additional features to be seen. (*a*) Genomic separation in the range from 0.1 to ~1.5 Mbp is correlated linearly to $<r^2>$ (Fig. 2 *B*). (*b*) The y-intercept of this relationship is approximately zero. (*c*) The slope of the relationship through points <2 Mbp is 1.9 μm²/Mbp. This slope is ~20-fold greater than the slope of the relationship through the points for genomic separations >10 Mbp (Fig. 2 *A*). (*d*) A marked decrease in slope is observed near 2 Mbp.

A Biphasic Relationship Is Also Observed in Alternatively Prepared Nuclei

The measurements shown in Fig. 2 were obtained on nuclei exposed to a hypotonic buffer, methanol/acetic acid fixative, and ethanol before FISH (hypo-MAA). Two experiments were performed to determine whether these pretreatments affect the spatial relationships among sequences in interphase chromosomes. In the first experiment, eight probe pairs, representing genomic separations ranging from 0.25 to 190 Mbp, were evaluated in nuclei that were not exposed to hypotonic buffer (data not

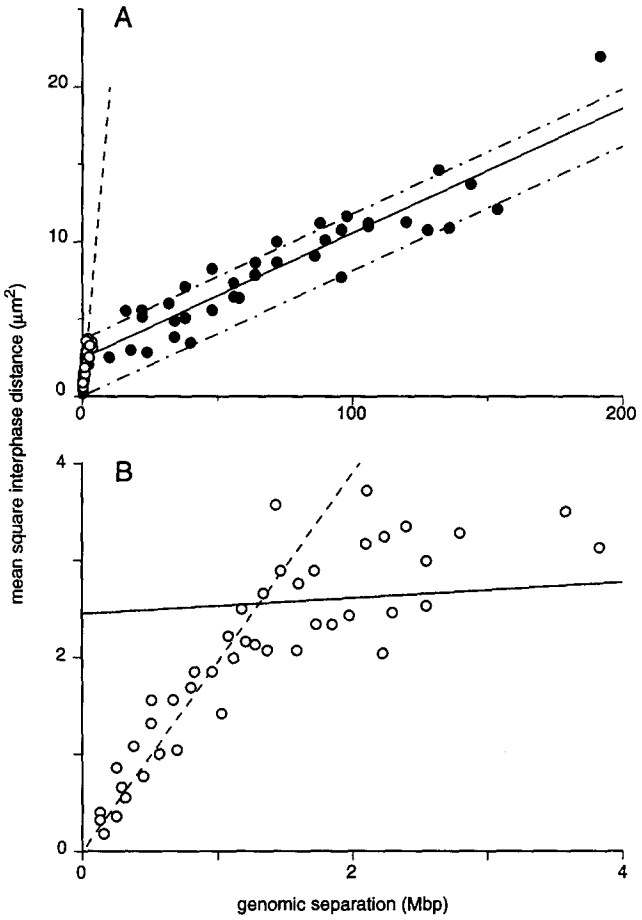

Figure 2. The relationship between the mean-square interphase distance, $<r^2>$, and genomic separation, *d*, for probes on chromosome 4. A total of 36 probe pairs in the 10–190 Mbp range (*black symbols*) and 44 probe pairs in the 0.1–4 Mbp range (*white symbols*) was analyzed using hypotonically swollen and methanol/acid fixed G0/G1 fibroblast nuclei (preparation 384). *A* shows the entire distance range; *B* shows an expanded view of values <4 Mbp. Each data point represents an average of 154 interphase distance measurements (range: 90–249). SEMs are not shown, but are ~4% of the mean. See legend to Fig. 1 for estimates of error in genomic separation values. Solid line is the best-fit linear regression line through the data points >10 Mbp. Dashed line is the best-fit linear regression line through the data points <1.5 Mbp. These two lines are shown for reference on both *A* and *B*. The two broken (*dash-dot*) lines refer to a random walk/giant loop model for interphase chromosome geometry (see Discussion and Sachs et al., 1995). According to the model there should be a "cloud" of points between the two broken lines.

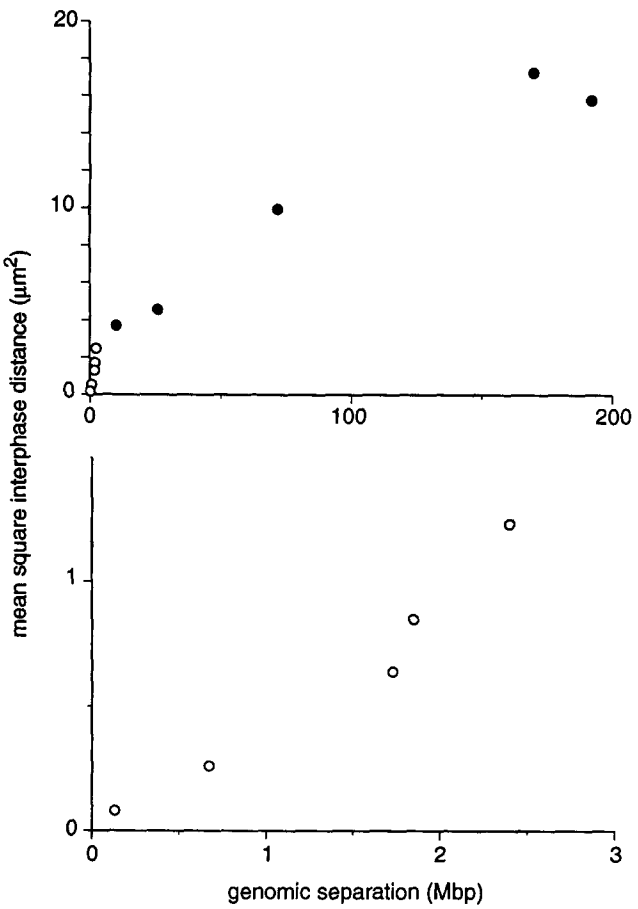

Figure 3. The relationship between mean-square interphase distance $<r^2>$, and genomic separation, *d*, in fibroblast cells grown on coverslips and fixed with paraformaldehyde. The nuclei were not exposed to hypotonic swelling, alcohols, or high concentrations of acid. The nuclei were hybridized with 10 probe pairs from chromosome 4, representing genomic separations from 0.15 to 190 Mbp. The bottom panel shows an expanded view of values <4 Mbp (open symbols in both panels). Errors are not shown, but are as described in legend to Fig. 2.

shown). In the second experiment, 10 probe pairs, representing genomic separations from 0.15 to 190 Mbp were evaluated in nuclei of cells grown on coverslips, fixed in situ with paraformaldehyde, permeabilized with Triton X-100, and subjected to three freeze–thaw cycles (Fig. 3). These nuclei were not exposed to methanol, ethanol, acid, or hypotonic swelling. Nuclear dimensions of paraformaldehyde nuclei were ~0.75 times shorter than those of hypo-MAA nuclei. The pattern of staining with DAPI, a DNA-specific fluorochrome, of paraformaldehyde-fixed nuclei is indistinguishable from that of unfixed nuclei and, after summation of optical sections to simulate physical projection, similar to hypo-MAA nuclei (not shown). Denaturation and FISH caused no noticeable changes in the DAPI staining pattern of the three preparations (not shown). Absolute mean distances were smaller in these two alternative nuclear preparations (~0.8- and ~0.7-fold), but relative probe-to-probe distances were similar to those observed in hypo-MAA nuclei. A marked biphasic relationship between mean-square interphase distance and genomic separation was observed regardless of preparation procedure (Fig. 3).

Measurements on Chromosomes 5 and 19 Confirm the Long Distance Observations on Chromosome 4

A linear relationship between $<r^2>$ and genomic separation, with a nonzero y-intercept, was also observed using probes distributed on chromosome 5 and chromosome 19 (8 and 7 probes, respectively) (Fig. 4). Using 42 probe combinations, the interphase proximity was determined of sequences separated by 15–180 Mbp on chromosome 5, and by 6–50 Mbp on chromosome 19. The slopes of the re-

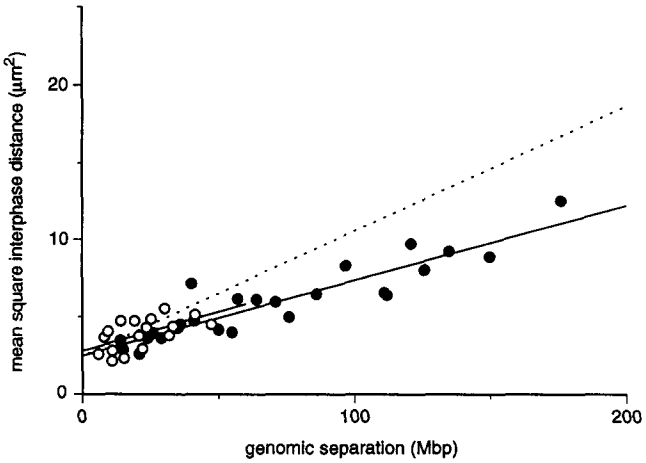

Figure 4. The relationship between mean-square interphase distance, $<r^2>$, and genomic separation, d, determined for human chromosomes 5 (*solid circles*) and 19 (*open circles*). A total of 25 probe pairs for chromosome 5 and 17 probe pairs for chromosome 19 was analyzed using nuclear preparation 384. Each data point represents an average of 165 interphase distance measurements (range: 50–226). Errors are not shown, but are as described in legend to Fig. 2. The solid lines are the best-fit linear regression lines through the data points on chromosomes 5 and 19, and the dotted line is the best-fit linear regression through the data points >10 Mbp on chromosome 4 (from Fig. 2).

lationships for chromosomes 5 and 19 are slightly lower (0.05 μm²/Mbp) than that observed for chromosome 4. As was the case for chromosome 4, the spread of the data points around the regression line is narrow and roughly constant across the entire genomic separation range on these chromosomes.

Statistical Distributions of Interphase Distance Follow Rayleigh Probability Densities

The linear relationship between $<r^2>$ and genomic separation for distances >10 Mbp suggests that the conformation of interphase chromatin on these large scales can be described by a polymer model, as is the case at smaller distances (van den Engh et al., 1992). Another test of polymer behavior can be made by evaluating the shape of the statistical distribution measured for each probe pair. Repetitive coordinate measurements between two points on the same polymer chain, with one point placed at the origin of a Cartesian coordinate system, are expected to form a bell-shaped (Gaussian) distribution centered at zero. The distributions of distances measured between the points after projection onto any plane are expected to follow what statisticians refer to as a Rayleigh distribution (Blank, 1980; Sachs et al., 1995). The Rayleigh distribution has a probability density of the form $P(r) = (r/\Gamma) \exp[-r^2/2\Gamma]$, where Γ is independent of r. Fig. 5 *A* shows the similarity between a Rayleigh distribution and a typical histogram of interphase distance measurements. The Rayleigh probability density has a specifically defined asymmetrical distribution that leads to characteristic ratios between means, mean-squares, medians, etc. (Sachs et al., 1995). For example, the Rayleigh distribution has a long right tail, which causes the median to be smaller than the mean by a factor

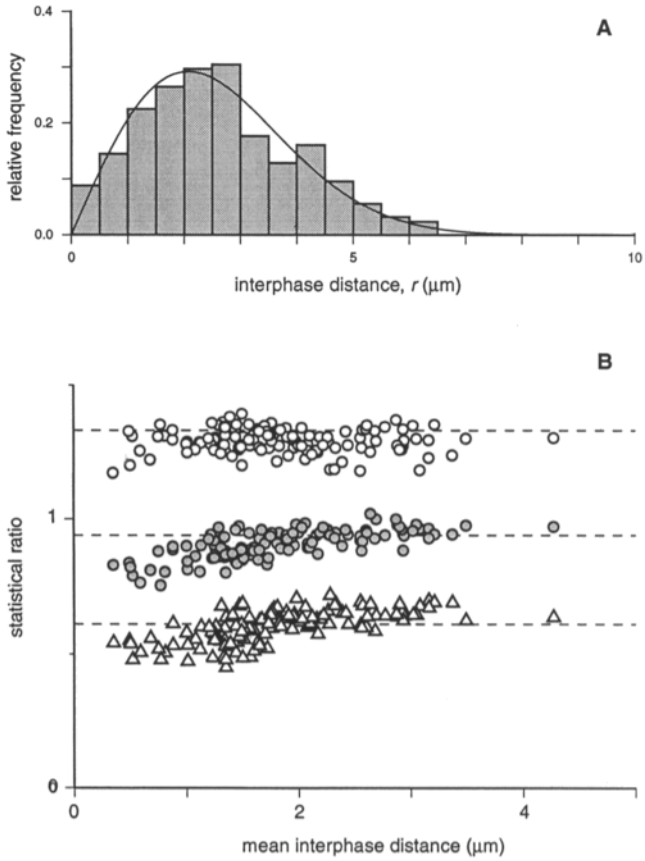

Figure 5. Comparisons of interphase distance distributions and the Rayleigh distribution. (*A*) Theoretical Rayleigh probability density (*line*) compared with a typical histogram of interphase distance measurements between two DNA sequence probes (*block histogram*). The parameter Γ in the Rayleigh function was adjusted to fit the raw data. The interphase distance distribution is the result of 249 measurements between E4 and C4–46, two probes ~65 Mbp apart on chromosome 4. (*B*) Statistical ratios derived from distributions of interphase distances and plotted as a function of mean interphase distance. These ratios characterize the shape of a probability density. The distributions analyzed are those measured for genomic separations ranging from 0.15 to 190 Mbp on chromosomes 4, 5, and 19 using hypotonically swollen, methanol/acid fixed nuclei. The ratios are third-quartile/mean (*white circles*), median/mean (*gray circles*), and first-quartile/mean (*triangles*). The predicted values for a Rayleigh distribution are shown as dotted lines: third-quartile/mean = 1.33, median/mean = 0.94; and first quartile/mean = 0.61.

of 0.94. To test whether our interphase distance measurements conform to a Rayleigh distribution, we calculated four characteristic ratios, standard deviation/mean, first quartile/mean, median/mean, and third quartile/mean, for all measured distributions. Fig. 5 *B* plots three of these shape parameters against mean interphase distance for the data generated on methanol/acetic acid–fixed nuclei (Figs. 2 and 4). The experimental data cluster around the expected values for a Rayleigh distribution, irrespective of mean interphase distance. Slight deviation from the Rayleigh distribution is observed at distances <1.5 μm, which corresponds to genomic separations <4 Mbp. Table I lists the shape parameters averaged over the distributions made for each of the three chromosomes for distances

Table I. Comparison of the Experimental Statistics of Interphase Distance Measurements and Rayleigh Probability Densities

	Data sets for genomic separations >10 Mbp						Theory	
Shape parameter	Chromosome 4 hypo-MAA 1	Chromosome 4 hypo-MAA 2	Chromosome 4 no hypo/MAA	Chromosome 4 no hypo/PFA	Chromosome 5 hypo-MAA 1	Chromosome 19 hypo-MAA 1	Rayleigh	Rigid, random orientation
	$n = 36$	$n = 36$	$n = 4$	$n = 5$	$n = 25$	$n = 17$		
SD/mean	0.51 ± 0.04	0.49 ± 0.05	0.54 ± 0.04	0.45 ± 0.05	0.48 ± 0.04	0.53 ± 0.05	0.52	0.28
First quartile/mean	0.62 ± 0.03	0.64 ± 0.05	0.59 ± 0.06	0.66 ± 0.08	0.65 ± 0.04	0.62 ± 0.04	0.61	0.84
Median/mean	0.93 ± 0.04	0.94 ± 0.03	0.92 ± 0.02	0.96 ± 0.02	0.95 ± 0.03	0.90 ± 0.04	0.94	1.10
Third quartile/mean	1.29 ± 0.04	1.28 ± 0.04	1.28 ± 0.08	1.29 ± 0.06	1.29 ± 0.05	1.29 ± 0.04	1.33	1.23

Four shape parameters were derived from the distributions of repeated measurements of the distance between two points. Listed are the averages and standard deviations of the ratios derived from n distributions measured on the indicated chromosomes and indicated nuclear preparation. hypo-MAA 1 and 2, hypotonically swollen, methanol/acetic acid–fixed (preparations 384 and 383); no hypo/MAA, methanol/acetic acid fixed, but not hypotonically swollen; no hypo/PFA, paraformaldehyde fixed, no hypotonic swelling or exposure to acids or alcohols. The column "Rayleigh" gives the statistical ratios predicted by a Rayleigh probability density, consistent with a model in which the two points are on a flexible, polymer structure (for more detail on the mathematical derivation of this prediction, see Sachs et al., 1995). The ratios in the column "Rigid, random orientation," given for comparison purposes, are predicted if the two points are at a fixed distance from each other on a rigid backbone; random orientation of the backbone in three dimensions results in a distribution of measurements in the two-dimensional plane of observation.

≥10 Mbp. Data obtained using four different preparations of nuclei are shown for chromosome 4. For all data on genomic separations >10 Mbp ($<r>$ >1.5 μm), the experimental values are very similar to the values characteristic for a Rayleigh distribution. Distributions measured on nuclei not exposed to hypotonic buffer, methanol, ethanol, or acetic acid also have Rayleigh characteristics.

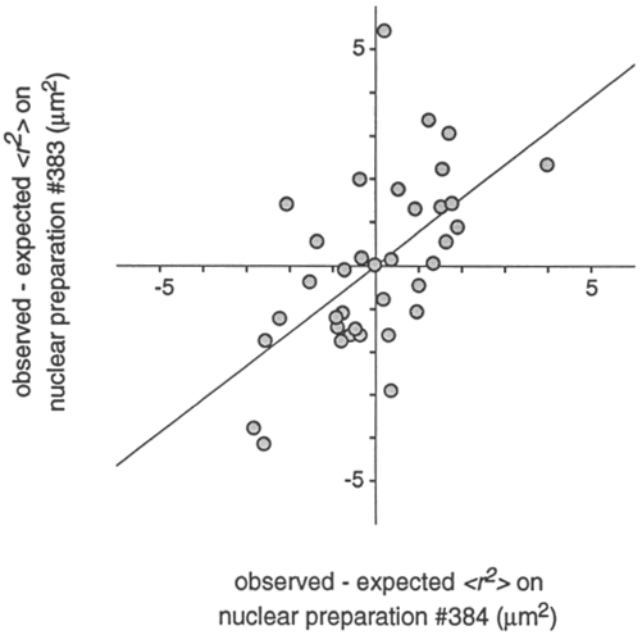

Figure 6. Reproducible deviation of data points above and below average trend of mean-square interphase distance and genomic distance. Mean-square interphase distance was measured on two different preparations of nuclei for 36 probe pairs representing genomic separations from 10 to 190 Mbp. The nuclei were prepared separately and independently. Nuclear preparation 384 was the one used for the measurements plotted in Figs. 2, 4, 5, and 7. For each genomic distance, the difference was calculated between the observed mean-square interphase distance and the average value, as defined by the linear regression line through all points (for nuclear preparation 384, solid line in Fig. 2). Thus, deviations are positive for data points above the linear regression line, and negative for points below the line. The deviation measured on one nuclear preparation is plotted against the deviation on the second preparation for each probe pair. The deviations in the two preparations are positively correlated ($P > 0.999$; $y = 0.776x + 0.001$; correlation coefficient $r = 0.581$; $n = 36$).

Data Points Are Reproducibly Positioned Relative to the Average Relationship of $<r^2>$ and Genomic Separation

The spread of data points around the regression lines in Figs. 2 and 4 is narrow and constant across the entire range of genomic separations. Although statistical error must account for some of this scatter pattern, we wished to determine if systematic positioning of the data points is responsible for some of the observed variation. Reproducibility in the position of data points above or below the average trend would be expected if probe sites are consistently positioned within a higher-order organizational structure. 36 probe pairs representing genomic distances ranging from 10 to 190 Mbp were analyzed on two, separately prepared batches of nuclei. For each genomic separation, we determined the deviations of individual $<r^2>$ from the linear regression line. Fig. 6 shows that the deviations observed in the two nuclear preparations are positively correlated. The slope is 0.776, the y-intercept is 0.001, and the correlation coefficient $r = 0.581$. With 36 observations, the correlation probability is >0.999.

Interphase Distances Can Decrease Locally with Increasing Genomic Separation

Although the overall correlation between $<r^2>$ and genomic separation in Figs. 2, 3, and 4 is positive, one would expect to observe local inversions in slope within this data cloud if chromatin is constrained periodically and particular DNA sequences occupy fixed positions in the resulting structure. We observed such an event using probes within a 4-Mbp region of Xq28 (Fig. 7). This region contains a 1-Mbp cluster of genes, including color vision and G6PD and two clones (p625 and p624) from the factor VIII gene, in that order (Kenwrick and Gitschier, 1989). Within the 1-Mbp cluster, $<r^2>$ increases in proportion to genomic separation (Fig. 7 *B*, *solid symbols*), with a slope very similar to that observed for chromosome 4 in this range. A negative correlation between interphase distance and genomic separation was found when we measured the dis-

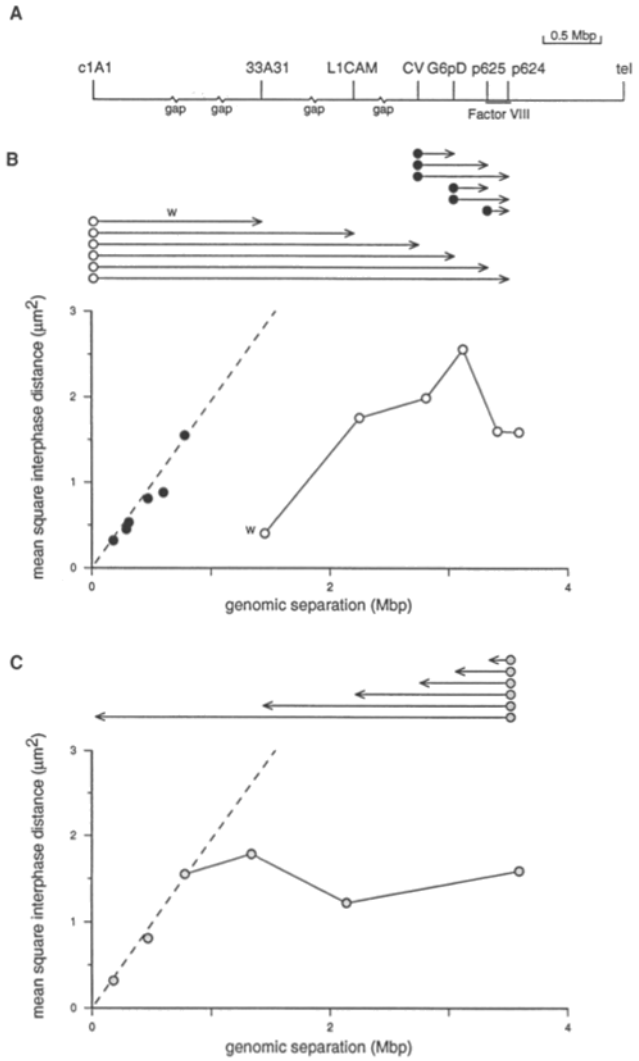

Figure 7. Evidence for local inversion in slope of the mean-square interphase distance vs. genomic separation graph. (*A*) The map of Xq28 shows the most recent estimates of probe spacing based on cosmid walking, sequence-tagged site–content mapping and fingerprinting of yeast artificial chromosomes, pulsed field gel electrophoresis and genetic linkage data (Kenwrick and Gitschier, 1989; Poustka et al., 1991; Schlessinger et al., 1991; Palmieri et al., 1994). Cosmids (~45 kbp) were used as probes to mark the sites of c1A1, 33A31, L1CAM, the color vision genes (*CV*), G6PD, and two portions of the factor VIII gene, p625 and p624. The cosmid representing CV hybridizes to a tandem array of CV genes spanning ≥120 kbp. (*B* and *C*) The relationship between mean-square interphase distance and genomic distance in Xq28 for a subset of probe pair combinations. Interphase distance measurements were made on the same preparation of nuclei used for Figs. 2 and 4 (preparation 384). The data points in *B* are shown as white circles or black circles to correspond to the most proximal probe used in each pairwise measurement. Black circles indicate interphase distances measured among probes within the 1-Mbp cluster of genes from the color vision locus to p624 in the factor VIII gene. Measurements from the most proximal probe, c1A1, are shown as white circles. The linear distance and data point for the pair c1A1 and 33A31 are marked with the letter w. Measurements made from p624 to probes located progressively more proximal on the chromosome are shown as gray circles in *C*. Each data point represents an average of 179 measurements (range: 90–254). Eight probe pairs were measured independently by two individuals; their mean-square values were averaged before plotting. SEMs are not shown, but are ~4% of the mean. In both *B* and *C*, the dashed line is the best-fit linear regression through the data points <1.5 Mbp for chromosome 4 and is the same as the dashed line in Fig. 2.

tance from points within this 1-Mbp cluster to a point known to lie significantly closer to the centromere, c1A1 (DXS374). The interphase distance measurements from c1A1 to the other Xq28 markers (nuclear preparation 384) and the generally accepted genomic separation estimates are plotted in Fig. 7 *B* (*open symbols*). With increasing genomic separation from c1A1, interphase distance first increases, and then decreases. In contrast, interphase distances from the most distal marker in the Xq28 map, p624, to points progressively closer to the centromere first increase and then, at separations >1 Mbp, appear to plateau (Fig. 7 *C*). In addition, c1A1 and 33A31 are very close to each other in interphase (mean = 0.55 μm), despite their separation on the linear DNA molecule of ≥1.45 Mbp.

These results confirm our earlier analyses of the folding of the Xq28 region in two other nuclear preparations (Trask et al., 1991). We reported previously that the factor VIII gene was consistently closer to the proximal markers, c1A1 and 33A31 (DXS134), than were the color vision genes (Trask et al., 1991). Since our original report, several lines of molecular and genetic evidence have been reported that convincingly support the reverse orientation (Poustka et al., 1991; Schlessinger et al., 1991; Palmieri et al., 1994) (Fig. 7 *A*). Thus, the Xq28 results demonstrate a situation in which interphase distance decreases as function of genomic separation.

Discussion

In the interphase nucleus, chromatin fibers follow a contorted path that cannot be followed directly. The folding of the fibers can be inferred by analyzing the two-dimensional, projected distances between DNA sequences whose positions on the linear DNA molecule are known. Our observations support a random walk/giant loop model for interphase chromatin and exclude some other models.

Random Walk/Giant Loop Model

The random walk/giant loop model is schematically illustrated in Fig. 8. Rigorous mathematical treatment of this model, with only three adjustable parameters, is provided by Sachs et al. (1995). Chromatin is organized in flexible, loose giant loops[2]. Within each loop, the chromatin follows a random path. The loops are formed by intrastrand protein connections linking sites that are several Mbp apart (Fig. 8, points *a* and *a'*). The connections form at or near the same DNA sequences in different cells. The "loop attachment points" themselves lie along a random

2. The giant loops are to be distinguished from the smaller loops, on a scale of <100 kbp, which are supported by molecular and structural studies (Benyajati and Worcel, 1976; Mirkovitch et al., 1984). We note that various local configurations, such as winding of DNA around histones, its packing into a 30-nm fiber, local alignment with lamina (Paddy et al., 1990), and chromatin loops <100 kbp, are too small in scale to be studied in interphase nuclei by FISH and light microscopy.

walk. We call the polymer-like path of the loop attachment points the "backbone."

Predictions of the Random Walk/Giant Loop Model

A chromatin model that involves two levels of random walk behavior leads to several predictions. The distance between points within a loop (Fig. 8, among points *c–f*) is expected to increase with a characteristic determined mainly by the properties of the loop chromatin. If chromatin folding within the loop is random, then mean-square interphase distance and genomic separation are linearly related over distances less than several Mbp. The distance between points close to the backbone (points *a* and *i*) is determined mainly by the characteristics of the backbone. If the backbone is a flexible, randomly folding structure, a linear relationship between mean-square interphase distance and genomic separation is again expected. The distance between points separated by several loops (points *a* and *j*) depends on their respective distances to the nearest loop attachment point and on the distance along the random walk between the loop attachment points.

Note that, over intermediate scales, interphase distance may inversely relate to separation along the looping DNA strand. The correct order is *c*, *d*, *e*, *f*, and *g* viewing from position *b*. Due to the loop structure, however, the mean-square physical distance between *b* and *g* will be shorter than that between *b* and *e*.

Measurements between randomly chosen points on the interphase chromosome are expected to yield a cloud of observations around a biphasic relationship. This cloud has three well-described boundaries. The lower extreme is determined by distances between points close to the backbone. This boundary has a slope determined by the random walk characteristic of the backbone and a y-intercept of approximately zero. The upper boundary is determined by pairs of points both midway in their respective loops; it runs parallel to the lower boundary, but is offset by a value characteristic for the loop size. If loops form consistently near specific DNA sequences, data points will be positioned reproducibly within the cloud. The cloud's leading edge is determined by point pairs on the same or adjacent loops. This relationship is linear, reflecting the polymer-like behavior of chromatin within the loops. The line defined by intraloop distances goes through the origin with a steeper slope than that defined by point pairs on the backbone. The boundaries for a random walk/giant loop structure with loops of ~3 Mbp have been calculated by Sachs et al. (1995) based on the data for chromosome 4. These theoretical envelopes are shown in Fig. 2.

Experimental Observations

Our data on human interphase chromosomes are in agreement with a giant loop/flexible backbone model. We demonstrate: (*a*) distance distributions that conform to the Rayleigh distribution, indicating overall random folding; (*b*) a striking biphasic relationship between mean-square interphase distance and genomic separation, indicating two levels of random walk polymer behavior; (*c*) a narrow and reproducible spread of data points around the biphasic relationship, consistent with the systematic positioning of DNA sequences within a periodic, higher order organization; and (*d*) an example where physical distance briefly decreases as genomic distance increases, indicative of a looped structure.

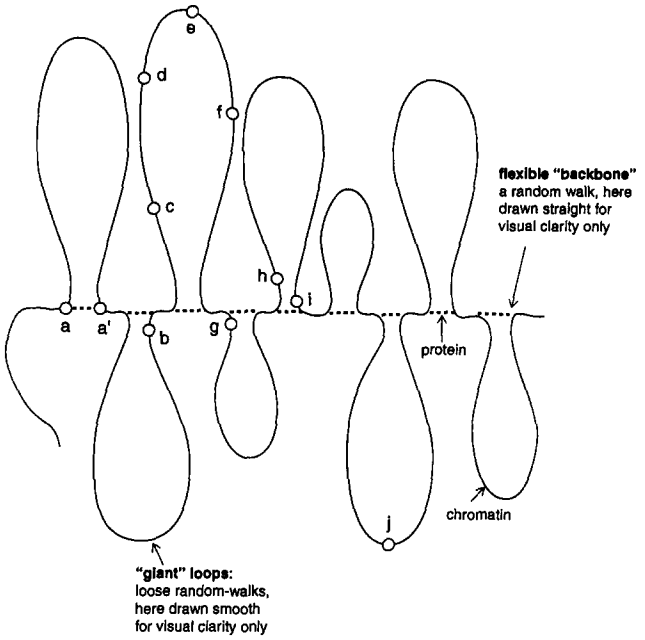

Figure 8. A random walk/giant loop model for interphase chromosomes. See Discussion for a detailed explanation, and Sachs et al. (1995) for a mathematical description. The chromatin follows a much longer, more tortuous path than the path schematically shown here. In the model, chromatin is organized in giant loops, i.e., loops containing several Mbp of DNA. Loop attachment points, such as *a* and *a'*, are connected by as yet unidentified proteins. Chromatin follows a loose, random walk within each loop. Loop attachment points also lie on a random walk, termed here the backbone. The relative length of the chromatin and protein portions of the backbone is unknown. Note that local configurations involving <100 kbp or <0.25 μm are too small in scale to appear in the figure or to be analyzed in interphase nuclei by FISH and light microscopy.

Statistics of Pair-wise Distance Measurements. The shape parameters of the distance distributions are one indication that the chromatin folds with a large degree of randomness. The experimental values on three different chromosomes closely match the shape parameters of the Rayleigh probability density, which is characteristic for random walks (Table I). Significantly, the shape parameters do not depend on genomic separation >10 Mbp (Fig. 5) or fixation method (Table I). Other distributions, such as one obtained by measuring between two points held a fixed distance apart in three dimensions, but projected randomly onto the measurement plane, yield very different values (Table I, last column).

Biphasic Relationship. The relationship of mean-square interphase distance ($<r^2>$) and genomic separation is biphasic (Figs. 2 and 3). For human chromosome 4, $<r^2>$ rises initially with a rate of 1.9 μm^2/Mbp. This relation changes abruptly around 2 Mbp to a second linear phase with a slope of 0.08 μm^2/Mbp extending to separations of ~200 Mbp. Data on chromosomes 5 and 19 are in general agreement with this picture (Fig. 4). The sharp transition indicates that chromatin follows a loose random walk path

for some number of steps, but is regularly constrained by connections between points several Mbp apart. Given the positive slope of the second phase, these connection points must also lie along a random walk path.

Reproducible Spread of the Data Points. The data points in Figs. 2 and 4 fall within a band of constant width around the regression lines, providing an important indication of a systematic, looped structure. Without systematic constraints, the spread of data points is expected to increase with increasing genomic separation. The excellent fit of the data within the theoretical boundaries (Fig. 2) supports the existence of sequence-specific, rather than random, loop attachment points. Moreover, measurements made on two, independent nuclear preparations are correlated (Fig. 6), indicating that some DNA sequences are systematically closer together or farther apart than the average for their genomic separation. This reproducible deviation is consistent with a model in which loops form relatively consistently near particular DNA sequences.

Local Inversion in Slope. Further support for giant loops comes from observations in Xq28 (Fig. 7). One interpretation for the close physical proximity, but large genomic separation, of c1A1 and 33A31 is that they both lie close to the backbone (Fig. 8, points *h* and *i*). A local inversion in slope is also observed in Xq28, as predicted by a model in which chromatin takes a path away from and then returns to a backbonelike structure. With increasing genomic separation from c1A1, interphase distance increases and then decreases (Fig. 7 *B*). This negative correlation suggests that c1A1 is near the backbone on one loop (Fig. 8, point *i*), and the other markers are on a neighboring loop (points *g–c*, with the color vision genes furthest from the backbone). Measurements made in the other direction from p624 increase and then briefly plateau as expected (i.e., *c* to *d–i*). This simple geometric configuration is consistent with the model based on our interpretation of Figs. 2–6. A "bend" in the interphase configuration of a 2.4-Mbp YAC observed by den Dunnen et al. (1992) is also consistent with this model.

Our results have implications for the use of interphase FISH for physical mapping (Trask and co-workers, 1991*b*, 1993*b*). Interphase distance will be most useful for estimating relative genomic separations <1 Mbp, where the relationship is steep. However, care should be exercised even when a clear probe order emerges in interphase; a looped configuration may invert the order relative to the sequence on the DNA molecule.

Nature of the Flexible Backbone

In the schematic representation of the model, the backbone is drawn as alternating protein links connecting points averaging ~3 Mbp apart and short chromatin links between neighboring loops. The chromatin links are analogous to, but on a much larger scale than, linker DNA between nucleosomes. We have no information regarding the relative lengths of the protein and DNA components of the proposed backbone. The protein links could be very short, in which case the backbone would be composed almost entirely of chromatin links as long as ~0.2 Mbp. Alternatively, the chromatin links could be very short, and the random walk properties of the backbone could depend primarily on the connective proteins. It may be possible to identify additional candidate loop attachments, sequences with interphase behavior analogous to c1A1's, and examine them for common sequence or protein affinity properties. It is tempting to speculate that the recently described coiled coil proteins, which have similarity to motor molecules (Strunnikov et al., 1993; Chuang et al., 1994; Hirano and Mitchison, 1994), might sit along the backbone and reel in the giant loops to form condensed mitotic chromosomes. It may not be coincidental that high resolution metaphase bands also contain ~3 Mbp of DNA.

Chromosome Domains in the Nucleus

Our measurements support the concept that the nucleus is partitioned into irregularly shaped chromosomal domains. Use of whole-chromosome paints has led to a similar conclusion, but concerns have lingered that these paints reveal the bulk of a chromosome and overlook its far-reaching, diffuse regions. By repeatedly measuring between specific points on a chromosome, we can determine the average size of its domain. Maximal intrachromosomal distances are short (4.5 μm) compared to nuclear dimensions (27 by 13 μm). Thus, a single chromosome does not expand to occupy the whole nuclear volume. The long distance scale factor of chromatin is ~0.065 μm^2/Mbp (average of chromosomes 4 and 5). For the whole genome, the corresponding area is 390 μm^2 (6×10^3 Mbp × 0.065 μm^2/Mbp), which, after accounting for z-axial overlap and interdigitation of domains, agrees well with an average nuclear area of 280 μm^2.

Intrachromosomal distances did not reach a plateau, as expected if chromosomal volume was restricted by external boundaries (Hahnfeldt et al., 1993). We find no evidence for a rigid, Rabl-like configuration of mammalian interphase chromosomes, as might have been anticipated from observations of prometaphase chromosomes in *Drosophila* (Hiraoka et al., 1990*a*). Given the random geometry of the chromosome as a whole, systematic compartmentalization within the chromosomal domain, for example in gene-rich and gene-poor subregions, as suggested by Cremer et al. (1993), also appears unlikely. Our findings do not preclude attachment of specific sequences to the nuclear matrix, envelope, or other nuclear components, but they indicate that these attachments do not constrain the chromosome into a nonrandom conformation.

Relevance of our Findings to the Organization of Chromosomes In Vivo

To obtain these data, FISH is used to label specific single-copy DNA sequences in fixed nuclei. The effects of fixation and FISH on nuclear structure are not completely understood. However, there are several indications why our observations may be a valid representation of the native organization. (*a*) Sequence-specific, systematic organization and reproducibility are observed characteristics likely to be inherent to the nuclei and unlikely to result from the fixation and FISH processes alone. (*b*) Hallmarks of random walk/giant loop organization (biphasic relationship and Rayleigh distributions) were found in three, alternatively fixed nuclear preparations. (*c*) It is unlikely that significant distortions in chromosomal geometry on scales

relevant to the giant loop and flexible backbone aspects of the model (>1 μm) could result from the fixation and FISH processes. Indeed, the DAPI staining pattern, a crude measure of gross nuclear morphology, was unchanged by denaturation and FISH. (*d*) The relative positions of homologous chromosomes, another measure of large-scale organization, are independent of fixation conditions (Hiraoka et al., 1993; Yokota, H., R. Sachs, G. van den Engh, and B. Trask, manuscript in preparation). It is formally possible that additional hierarchical levels exist in vivo on scales >100 kbp, with FISH selectively eliminating these organizational levels, but leaving evidence for giant loops. The difficult issues that arise in relating prepared samples to in vivo configurations will undoubtedly take time to resolve, as has been the case in studies of smaller-scale chromatin structure (van Holde, 1989) or mitotic chromosome structure (e.g., Rattner and Lin, 1985).

Conclusions

We have shown that measurements between the sites of specific DNA sequences give quantitative information about the large-scale geometry of chromatin during the G0/G1 phase of the cell cycle. For the three chromosomes studied, the data indicate two, and apparently only two, levels of higher-order chromatin structure at scales >0.15 Mbp. The simplest model that fully describes the spatial relationships we observe is that of flexible chromatin loops of several Mbp arranged along a tighter chromosomal backbone. Folding within each loop and of the backbone is dominated by random influences. Other models discussed by Sachs et al. (1995) are also consistent with the data, but are more complicated and require additional parameters for their description.

Our description of chromatin folding is the first step in understanding how large-scale structure affects or is affected by cellular processes. Further elucidation of interphase organization will require detailed maps and associated DNA clones. For example, measurements among probes placed every ~200 kbp for spans of ~10 Mbp are needed to support further discussions about the sequence specificity of loop formation, or to determine if regional differences exist in loop size or compaction. A future challenge will be to determine the composition and relative contribution of the protein and chromatin links between loops to the total length of the backbone random walk. Further intrachromosomal measurements may also help us to understand how chromosomes decondense and recondense during the cell cycle or how interphase geometry is affected by transcriptional activity.

We thank the colleagues named in Materials and Methods for generously providing probes for our study, Anne-Marie Poustka (Deutsches Krebsforschungszentrum, Heidelberg, FRG) and David Schlessinger (Washington University, St. Louis, MO) for communicating unpublished Xq28 map information, Michael Botchan (University of California, Berkeley, CA) for critically reading an earlier version of the manuscript, and, at the University of Washington, Myron Peto, Hillary Massa, and Cynthia Friedman for technical assistance, and Richard Esposito and Brian Pinkerton for developing software for interfacing a computer to the digitizing board and data analysis. We also thank Tom Donnelly at Applied Precision, Inc., for advice and access to the DeltaVision instrument.

This work was supported by National Institutes of Health (NIH) grant R01 HG00256 and United States Department of Energy grant FG06-93ER61553 (to B. J. Trask), NIH grant R01 GM47945-03 (to J. E. Hearst), and National Science Foundation grant DMS-930-2704 (to R. K. Sachs).

Received for publication 13 December 1994 and in revised form 2 June 1995.

References

Agard, D. A., Y. Hiraoka, P. Shaw, and J. W. Sedat. 1989. Fluorescence microscopy in three dimensions. *Methods Cell Biol.* 30:353–377.

Bates, G. P., M. E. MacDonald, S. Baxendale, Z. Sedlacek, S. Youngman, D. Romano, W. L. Whaley, B. A. Allitto, A. Poustka, J. F. Gusella, and H. Lehrach. 1990. A yeast artificial chromosome telomere clone spanning a possible location of the Huntington disease gene. *Am. J. Hum. Genet.* 46:762–775.

Benyajati, C., and A. Worcel. 1976. Isolation, characterization, and structure of the folded interphase genome of *Drosophila melanogaster*. *Cell.* 9:393–407.

Blank, L. 1980. Statistical Procedures for Engineering, Management and Science. McGraw-Hill, New York. 649 pp.

Blobel, G. 1985. Gene gating: A hypothesis. *Proc. Natl. Acad. Sci. USA.* 82: 8527–8529.

Buçan, M., M. Zimmer, W. L. Whaley, A. Poustka, S. Youngman, B. A. Allitto, E. Ormondroyd, B. Smith, T. M. Pohl, M. MacDonald, et al. 1990. Physical maps of 4p16.3, the area expected to contain the Huntington disease mutation. *Genomics.* 6:1–15.

Cantor, C. R., and P. R. Schimmel. 1980. Biophysical Chemistry. W. H. Freeman, San Francisco. 2558 pp.

Chuang, P.-T., D. G. Albertson, and B. J. Meyer. 1994. DPY-27: a chromosome condensation protein homolog that regulates *C. elegans* dosage compensation through association with the X chromosome. *Cell.* 79:389–392.

Comings, D. E. 1968. The rationale for an ordered arrangement of chromatin in the interphase nucleus. *Am. J. Hum. Genet.* 20:550–560.

Cook, P. R. 1991. The nucleoskeleton and the topology of replication. *Cell.* 66: 627–635.

Cremer, T., A. Kurz, R. Zirbel, S. Dietzel, B. Rinke, E. Schrock, M. R. Speicher, U. Mathieu, A. Jauch, P. Emmerich, et al. 1993. Role of chromosome territories in the functional compartmentalization of the cell nucleus. *Cold Spring Harbor Symp. Quant. Biol.* 58:777–792.

De Boni, U. 1994. The interphase nucleus as a dynamic structure. *Int. Rev. Cytol.* 150:149–171.

Den Dunnen, J. T., P. M. Grootscholten, J. G. Dauwerse, A. P. Walker, A. P. Monaco, R. Butler, R. Anand, A. J. Coffey, D. R. Bentley, H. Y. Steensma, et al. 1992. Reconstruction of the 2.4 Mbp human DMD-gene by homologous YAC recombination. *Hum. Mol. Genet.* 1:19–28.

Doi, M., and S. F. Edwards. 1988. The Theory of Polymer Dynamics. Oxford University Press, Oxford, UK. 391 pp.

DuPraw, E. J. 1965. Macromolecular organization of nuclei and chromosomes: a folded fibre model based on whole-mount electron microscopy. *Nature (Lond.).* 206:338–343.

Flory, P. J. 1988. Statistical mechanics of chain molecules. Oxford University Press, New York. 432 pp.

Hahnfeldt, P., J. E. Hearst, D. J. Brenner, R. K. Sachs, and L. R. Hlatky. 1993. Polymer models for interphase chromosomes. *Proc. Natl. Acad. Sci. USA.* 90:7854–7858.

Hirano, T., and T. J. Mitchison. 1994. A novel coiled-coil protein required for mitotic chromosome condensation in vitro. *Cell.* 79:449–458.

Hiraoka, Y., D. Agard, and J. W. Sedat. 1990*a*. Temporal and spatial coordination of chromosome movement, spindle formation, and nuclear envelope breakdown during prometaphase in *Drosophila melanogaster* embryos. *J. Cell Biol.* 111:2815–2828.

Hiraoka, Y., J. W. Sedat, and D. A. Agard. 1990*b*. Determination of the three-dimensional imaging properties of an optical microscope system: partial confocal behavior in epifluorescence microscopy. *Biophys. J.* 57:325–333.

Hiraoka, Y., A. F. Dernburg, S. J. Parmelee, M. C. Rykowski, D. A. Agard, and J. W. Sedat. 1993. The onset of homologous chromosome pairing during *Drosophila melanogaster* embryogenesis. *J. Cell Biol.* 120:591–600.

Johnson, G. D., and G. M. Noguera-Araujo. 1981. A simple method of reducing the fading of immunofluorescence during microscopy. *J. Immunol. Methods.* 43:349–350.

Kenwrick, S., and J. Gitschier. 1989. A contiguous, 3-Mb physical map of Xq28 extending from the color-blindness locus to DXS15. *Am. J. Hum. Genet.* 45: 873–882.

Lawrence, J. B., and R. H. Singer. 1991. Spatial organization of nuclei acid sequences within cells. *Semin. Cell Biol.* 2:83–101.

Lewin, B. 1994. Chromatin and gene expression: constant questions, but changing answers. *Cell.* 79:397–406.

Lichter, P., T. Cremer, J. Borden, L. Manuelidis, and D. C. Ward. 1988. Delineation of individual human chromosomes in metaphase and interphase cells by in situ suppression hybridization using recombinant DNA libraries. *Hum. Genet.* 80:224–234.

Lin, C. S., M. Altherr, G. Bates, W. L. Whaley, A. P. Read, R. Harris, H. Lehrach, J. J. Wasmuth, J. F. Gusella, and M. E. MacDonald. 1991. New DNA markers in the Huntington's disease gene candidate region. *Somatic Cell Mol. Genet.* 17:481–488.

Lu-Kuo, J. M., D. Le Paslier, J. Weissenbach, I. Chumakov, D. Cohen, and

D. C. Ward. 1994. Construction of a YAC contig and a STS map spanning at least seven megabasepairs in chromosome 5q34-35. *Hum. Mol. Genet.* 3:99–106.

Manuelidis, L., and T. L. Chen. 1990. A unified model of eukaryotic chromosomes. *Cytometry.* 11:8–25.

Mirkovitch, J., M.-E. Mirault, and U. K. Laemmli. 1984. Organization of the higher-order chromatin loop: specific DNA attachment sites on nuclear scaffold. *Cell.* 39:223–232.

Myers, R., and R. Goold. 1992. Human Genome Mapping Center Newletter, Vol. 1, April, 1992.

Ostashevsky, J. Y., and C. S. Lange. 1994. The 30-nm chromatin fiber as a flexible polymer. *J. Biomol. Struct. & Dyn.* 11:813–820.

Paddy, M. R., A. S. Belmont, H. Saumweber, D. A. Agard, and J. W. Sedat. 1990. Interphase nuclear envelope lamins form a discontinuous network that interacts with only a fraction of the chromatin in the nuclear periphery. *Cell.* 62:89–106.

Palmieri, G., G. Romano, A. Ciccodicola, A. Casamassimi, C. Campanile, T. Esposito, V. Cappa, A. Lania, S. Johnson, R. Reinbold, et al. 1994. YAC contig organization and CpG island analysis in Xq28. *Genomics.* 24:149–158.

Pinkel, D., J. Landegent, C. Collins, J. Fuscoe, R. Seagraves, J. Lucas, and J. W. Gray. 1988. Fluorescence in situ hybridization with human chromosome-specific libraries: detection of trisomy 21 and translocations of chromosome 4. *Proc. Natl. Acad. Sci. USA.* 85:9138–9142.

Popp, S., H. P. Scholl, P. Loos, A. Jauch, E. Stelzer, C. Cremer, and T. Cremer. 1990. Distribution of chromosome 18 and X centric heterochromatin in the interphase nucleus of cultured human cells. *Exp. Cell Res.* 189:1–12.

Poustka, A., A. Dietrich, G. Langenstein, D. Toniolo, S. T. Warren, and H. Lehrach. 1991. Physical map of Xq27-Xqter: localizing the region of the fragile X mutation. *Proc. Natl. Acad. Sci. USA.* 88:8302–8306.

Rabl, C. 1885. Uber Zellteilung. *Morphologisches Jahrbuch.* 10:214–330.

Rattner, J. B., and C. C. Lin. 1985. Radial loops and helical coils coexist in metaphase chromosomes. *Cell.* 42:291–296.

Sachs, R. K., G. van den Engh, B. J. Trask, H. Yokota, and J. E. Hearst. 1995. A random-walk/giant-loop model for interphase chromosomes. *Proc. Natl. Acad. Sci. USA.* 92:2710–2714.

Schlessinger, D., R. D. Little, D. Freije, F. Abidi, I. Zucchi, G. Porta, G. Pilia, R. Nagaraja, S. K. Johnson, J. Y. Yoon, et al. 1991. Yeast artificial chromosome-based genome mapping: some lessons from Xq24-Xq28. *Genomics.* 11: 783–793.

Strunnikov, A. V., V. L. Larionov, and D. Koshland. 1993. *SMC1*: an essential yeast gene encoding a putative head-rod-tail protein is required for nuclear division and defines a new ubiquitous protein family. *J. Cell Biol.* 123:1635–1648.

Trask, B. J. 1991*a*. DNA sequence localization in metaphase and interphase cells by fluorescence in situ hybridization. *Methods Cell Biol.* 35:3–35.

Trask, B. J. 1991*b*. Fluorescence in situ hybridization: applications in cytogenetics and gene mapping. *Trends Genet.* 7:149–154.

Trask, B. J., D. Pinkel, and G. J. van den Engh. 1989*a*. The proximity of DNA sequences in interphase cell nuclei is correlated to genomic distance and permits ordering of cosmids spanning 250 kilobase pairs. *Genomics.* 5:710–717.

Trask, B. J., G. van den Engh, B. Mayall, and J. W. Gray. 1989*b*. Chromosome heteromorphism quantified by high resolution bivariate flow karyotyping. *Am. J. Hum. Genet.* 45:738–752.

Trask, B. J., H. Massa, S. Kenwrick, and J. Gitschier. 1991. Mapping of human chromosome Xq28 by 2-color fluorescence in situ hybridization of DNA sequences to interphase cell nuclei. *Am. J. Hum. Genet.* 48:1–15.

Trask, B. J., S. Allen, H. Massa, A. Fertitta, R. Sachs, G. J. van den Engh, and M. Wu. 1993*a*. Studies of metaphase and interphase chromosomes using fluorescence in situ hybridization. *Cold Spring Harbor Symp. Quant. Biol.* 58: 767–775.

Trask, B. J., A. Fertitta, M. Christensen, J. Youngblom, A. Bergmann, A. Copeland, P. de Jong, H. Mohrenweiser, A. Olsen, A. V. Carrano, and K. Tynan. 1993*b*. Fluorescence in situ hybridization mapping of chromosome 19: Cytogenetic band location of 540 cosmids and 70 genes or DNA markers. *Genomics.* 15:133–145.

van den Engh, G., R. Sachs, and B. J. Trask. 1992. Estimating genomic distance from DNA sequence location in cell nuclei by a random walk model. *Science (Wash. DC).* 257:1410–1412.

Van Holde, K. E. 1989. Chromatin. Springer Verlag, New York. 497 pp.

Whaley, W., G. Bates, A. Novelletto, Z. Sedlacek, S. Cheng, D. Romano, E. Ormondroyd, B. Allitto, C. Lin, S. Youngman, et al. 1991. Mapping of cosmid clones in Huntington's disease region of chromosome 4. *Somatic Cell Mol. Genet.* 17:83–91.